Figure Captions

Figure 1 Schematic diagram of the atomic geometry of C
the surface cell and its reciprocal lattice v
the associated diffraction pattern [Panel(b)]
primitive surface unit cell vectors is taken t
The beam positions are shown as if intersecti
detector symmetrically positioned about the i

Conf-901035--16

PNL-SA--18362

DE91 006723

LOW ENERGY POSITRON DIFFRACTION FROM Cu(111): IMPORTANCE OF SURFACE LOSS PROCESSES AT LARGE ANGLES OF INCIDENCE

October 1990

D. L. Lessor
C. B. Duke
P. N. Lippel
G. R. Brandes
K. F. Canter
T. N. Horsky

Presented at the
American Vacuum Society 37th National Symposium
October 8-12, 1990
Toronto, Canada

Work supported by the
U. S. Department of Energy
under Contract DE-AC06-76RLO 1830

Pacific Northwest Laboratory
Richland, Washington 99352

MASTER

LOW ENERGY POSITRON DIFFRACTION FROM CU(111): IMPORTANCE OF SURFACE LOSS PROCESSES AT LARGE ANGLES OF INCIDENCE

D. L. Lessor
Pacific Northwest Laboratory[a)]
P.O. Box 999, Richland, WA 99352

C. B. Duke
Xerox Webster Research Center
800 Phillips Road, 0114-38D
Webster, NY 14580

P.H. Lippel[b)], G.R. Brandes[c)], K.F. Canter, and T.N. Horsky[d)]

Department of Physics, Brandeis University[e)]
Waltham, Massachusetts 02254

ABSTRACT

Intensities of positrons specularly diffracted from Cu(111) were measured at the Brandeis positron beam facility and analyzed in the energy range 8eV<E<134eV for angles of incidence θ = 25, 30, 35, 40, 45, 50, 52, 57, and 60 degrees. These intensities were calculated for the known geometry of Cu(111) using a dynamical multiple scattering methodology. Above E = 50eV this methodology gives a useful account of the measured intensities using a constant imaginary optical potential of V_i = 4eV. At lower energies strong energy dependences occur associated both with multiple elastic scattering phenomena within atomic layers of Cu parallel to the surface and with the thresholds of inelastic channels (e.g., plasmon creation). Use of the free electron calculation of V_i shows that energy dependence of inelastic processes is necessary to obtain a satisfactory description of the absolute magnitude of the diffracted intensities below E = 50eV. Detailed comparison of the calculated and observed diffraction intensities reveals the necessity of incorporating surface loss processes explicitly into the model in order to achieve a quantitative description of the measured intensities for E<40eV and θ>40°.

I. INTRODUCTION

In recent years low-energy positron diffraction (LEPD) intensities have revealed themselves to be amenable to quantitative analysis analogous to low-energy electron diffraction (LEED) intensities.[1-5] Moreover, LEPD has been utilized to determine the atomic geometries of the cleavage faces of CdSe[6,7] in parallel with LEED, and the differences between the two have been analyzed.[5,7,8] These data and analyses have spanned a limited range of angles of incidence and beam energies, however, being largely confined either to high energies[1-4] or near-normal incidence[6,7] for which bulk inelastic loss processes are expected to dominate the imaginary part of the optical potential used to analyze the measured intensities.[9-12] Our purpose in this paper is to examine the adequacy of a model calculation based on bulk loss processes alone for the description of LEPD intensities from Cu(111) at low energies ($E<50eV$) and at high angles of incidence ($30° \leq \theta \leq 60°$). A schematic diagram of the Cu(111) surface geometry and the resulting positron diffraction pattern is given in Figure 1. We also test for the existence of intralayer scattering resonances[13,14] at low energies ($E<30eV$) because the small or negative real inner potential for positrons should render these resonances directly observable in the measured diffracted intensities. Surface barrier resonances have been predicted[15,15] at low energies, but either the inelastic collision damping is too large or the resolution of the data is too low to observe them in our data.

We proceed by outlining the procedures used to obtain the LEPD data in Section II and the calculation of the LEPD intensities in Section III. Section IV consists of a comparison of the calculated and measured intensities for the specularly reflected beam. A discussion of the origins of the discrepancies between the two is given in Section IV. The paper concludes with a synopsis.

II. EXPERIMENTAL PROCEDURES

A monoenergetic positron beam of 2mm diameter and 2° divergence over the energy range 5 - 200 eV was obtained from a Co-58 positron source and W(110) moderator followed by two stages of reflection-mode brightness enhancement.[17] The Cu(111) samples were treated in UHV (2×10^{-10} torr) with ion bombardment and annealing cycles. Auger analysis was used to ensure that the surfaces

remained clean with less than 2% of a monolayer contamination over the duration of each measurement, which is sufficient to make the beam intensity profiles essentially invariant to surface contamination during a run. The method of detecting the scattered, as well as the incident positron beam, is discussed in detail in Ref. 18. Briefly, a channel electron multiplier array with a position sensitive resistive channel encoder was placed to the side of the beam axis and positrons were scattered/diffracted into the detector. Using suppressor grids on the detector and monitoring the diffracted positron angular distribution ensured that we could accurately measure the specular (00) diffracted beam over the incident beam 5 - 200 eV interval. The incident beam flux as a function of energy was monitored with the same detector array by swinging an electrostatic mirror into the beam line, in the sample position, and recording the mirrored counts versus incident energy. By dividing the diffracted beam counts by the mirrored counts we were able to obtain accurate diffraction intensities (I-V profiles) without having to know the detector efficiency as a function of energy. Data was obtained in a multiscaling mode with a typical energy scan being repeated at least ten times to minimize any possible beam drift effects.

III. MODEL CALCULATIONS

An approximate multiple-scattering model of the low-energy position diffraction process[3] was used to calculate the diffracted intensities. This model is embodied in a series of computer programs in which the scattering species are represented by phase shifts in terms of which the LEPD intensities from the surface are evaluated. The scattering amplitudes associated with the uppermost few atomic layers are evaluated exactly, as are those of each of the individual atomic layers beneath. These amplitudes are superposed and weighted by appropriate phase factors to obtain the diffracted intensities. Convergence tests are utilized to determine the dependence of the calculated intensities on the total number of atomic layers, the number of atomic layers in which multiple scattering is treated exactly, and the number of phase shifts used to describe the electron-ion-core scattering. Twelve atomic layers were used throughout. Typically the scattering within the uppermost six are treated exactly but for $E<40eV$ we often extended this treatment to as many as nine top layers, as required.

The positron-ion-core interaction is described by a one-electron muffin-tin potential. The crystal potential is formed from a superposition of overlapping atomic electronic charge densities. These charge densities are obtained via self-consistent solutions to the Dirac equation for the individual atomic species.[19,20] Given the charge densities, the phase shifts are evaluated by solving the Schrodinger equation for positrons without exchange. A muffin-tin approximation to the crystal potential is imposed prior to the calculation of the phase shifts. Details of the calculational procedure are given by Weiss et al.[3] A comparison of the resulting potentials and phase shifts with the corresponding ones for electrons is presented by Duke and Lessor.[8]

The electron-positron interaction is incorporated into our model via a complex inner potential well with constant real and imaginary parts, V_o and V_i respectively. For incident positron energies above E = 40eV the values V_o=0 and V_i=4eV yield good descriptions of the observations, as suggested by an earlier analysis of a more limited set of data.[3] We also calculated the diffracted intensities using values of V_i obtained from the positron self-energy calculation of Oliva.[10] Above E = 40eV this model predicts intensities comparable to those obtained using V_i=4eV, but near and below the plasmon emission threshold the predictions of the two models differ significantly.

The atomic geometry of the surface unit cell is given in Figure 1. The layer spacings are taken from the LEED analysis of Lindgren et al.[21] Lattice vibrations were taken into account by renormalizing the positron atom-core vertex with the use of a Debye-Waller factor.[22,23] The calculations were made with squared lattice vibration amplitudes corresponding to a Debye temperature (θ_D) of 343 K and a temperature (T) of 300K.

IV. COMPARISON OF MEASURED AND CALCULATED INTENSITIES

The first task that confronted us in initiating a new calculation for Cu(111) was the verification that we recovered the results of prior analyses. In Figure 2 we show a comparison of our calculated specular reflected intensities with the previously published data at an angle of incidence θ=30° and azimuthal angle of ϕ=60° reported by Rosenberg, Weiss, and Canter[24] and by Weiss et al.[3] Weiss et al[3] described their calculated intensities as providing a good representation not only of the measured intensities for

E>40eV but also of prior calculations by Jona et al[1] and by Read and Lowy.[2] The calculations of Weiss et al[3] are reproduced exactly for the V_i=4eV model (solid curve in Figure 2). Differences between experiment and calculation above 140 eV may be attributable to an unsubtracted background. The calculations using a model embodying V_i obtained from Oliva[10] (cross-dashed curves in Figure 2) provide a comparable representation of the data with some small differences in isolated energy regions (e.g., near E=70eV and 180eV). Overall, Figure 2 reveals that our present (fully converged) calculations reproduce quantitatively prior results using both of the "standard" models in the literature, as described in Section III.

Given our recovery of prior results, we next examined the extent to which our two "standard" models, i.e., V_i=4eV and V_i obtained from Oliva,[10] describe specular diffraction for larger angles of incidence. New data, at an azimuthal angle of ϕ=24° rather than ϕ=60°, were obtained for this purpose at θ = 25°, 30°, 35°, 40°, 45°, 50°, 52°, 57°, and 60°. More extensive data were obtained at θ = 30°, 40°, 50°, and 57° than at the other angles of incidence, so we show the analysis of these data in the figures presented herein.

The results of our analysis for E≥30eV are shown in Figure 3. Qualitatively they are comparable to those shown in Figure 2 (for ϕ=60°) although not so good in detail as for that high symmetry azimuth (possibly due to small errors in ϕ or θ in the experimentally measurements and/or the finite acceptance angles of the detector). An important result from Figure 3 is the use of different scaling factors, f, of the calculated to experimental curves in Figure 3 at different values of θ. Specifically, f = 1.0, 0.5, 0.18, and 0.13 for θ = 30°, 40°, 50°, and 57°, respectively. These visually determined multipliers are presented in Table 1, along with multipliers determined to minimize the integral of square of the difference between experimental and scaled calculated curves, and also the single beam X-ray R factors for the specular beam.[25] The sets of multipliers are comparable and compatible with an inelastic process that becomes more important with increasing departure from normal incidence, while the R factor values are in the range traditionally associated in LEED with reasonable agreement on curve shape.

The comparisons between measured and calculated intensities for lower energies, 10eV $\leq E \leq$ 40eV are, not unexpectedly, far less satisfactory as shown in Figure 4. The positron mean free path is rising rapidly with decreasing energy in this region, so the V_i = 4eV model is inappropriate since V_i is related to the mean free path, λ via[9,13]:

$$V_i = h^2 [2m(E+V_o) / h^2]^{1/2}/2m\lambda \qquad (1)$$

so that a constant V_i gives λ = const x $E^{1/2}$. The Oliva (free-electron) model which includes the bulk plasmon-emission threshold is, however, not much better in this energy range. Both models fail to give an energy and θ dependence of V_i compatible with the measurements in the low-energy range: a result which, while not unexpected, requires discussion in the following section.

V. DISCUSSION

The comparisons of the standard model calculations with the observed intensities, while qualitatively adequate at E$\geq$30eV, nevertheless, reveal two shortfalls of these two models. First, even for E$\geq$ 30eV a θ-dependent scaling of the calculated intensities is required for a quantitative description of the data for θ>30°. Second, the energy dependence of the observed intensities is poorly reproduced for E$\leq$30eV. In this section we consider each of these issues in turn.

The failure of the standard models to predict a decrease in the scaling factor f with increasing θ is a symptom of their inclusion only of bulk loss processes. For large values of θ, the creation of surface plasmons is an obviously important loss process which is not incorporated in the model.[26] Another important loss process which is not included in the model is the formation of positronium, i.e., the electron-positron bound state that can be formed as a result of electron capture by the positron as it leaves the metal surface.[27,28] In particular, Gidley et al. have shown that positronium formation is enhanced for positrons that scatter from metals when the positrons are directed at the surface at near grazing angles.[29] This is in keeping with the standard picture that positronium formation becomes more likely for positrons that spend a larger fraction of their time passing through the electron salvage where positronium formation is not prevented by high density

electron screening. Therefore, the primary implication of Figure 3 is the adequacy of the standard model once the loss of positrons to surface loss processes in the entrance and exit beams is incorporated into the calculation.

The failure of the standard models to reproduce the observed energy dependence of the specular diffracted positrons below E = 30eV also can be attributed in part to the neglect of surface-plasmon and positronium creation in the calculation of V_i. Moreover, the effective value of V_o in the surface region also is influenced by these phenomena[26] so these models may require extension to encompass spatially dependent (and probably non-local) inner potentials.[30] In addition, the free-electron model of Oliva is inappropriate for nobel metals like Cu so a more realistic model of bulk loss processes is required.

Another issue of importance in the low-energy region is that of diffraction resonances. Surface barrier resonances, i.e., multiple scattering resonances between the changes in electronic potential in the surface region and the ion core lattice, are expected[15,16] in this energy range, although the resolution of our data is too poor for us to detect them. Another important class of surface diffraction resonances consists of those due to multiple scattering within a given layer of scatterers parallel to the surface, i.e., intralayer scattering resonances.[13,14] The calculated intensities of positrons diffracted from a single atomic Cu(111) layer with a long mean free path within the layer are indicated in Figure 5. The intralayer scattering resonances evidently occur in the neighborhood of $4eV \leq E \leq 15eV$ and $25eV \leq E \leq 35eV$. Both are evident, if muted, in the V_i=4eV standard model calculation shown in Figure 4. Neither account for the large observed maximum in the reflected intensities in the vicinity of $10eV \leq E \leq 17eV$ evident in Figure 4. Thus, we attribute this peak to the net effect of diffraction in the presence of thresholds of inelastic channels in this energy region, with one inelastic threshold lying below 10eV and another around 12eV.

VI. SYNOPSIS

Analysis of specularly reflected positrons from Cu(111) over a wide range of incident angles ($25° \leq \theta \leq 60°$) reveal that standard models of the diffraction process, routinely used in LEPD and LEED structure analyses in the literature, give a qualitatively correct energy dependence of these intensities for $E \geq 40eV$,

but with a θ-dependent multiplier to scale theory to experiment. Hence these models suffice for the purpose for which they were constructed, i.e., structure analyses on the basis of examining multiple diffracted beams for positrons incident near the normal to the surface being examined. Accurate evaluation of the absolute diffraction intensities at different values of θ for $\theta \geq 30°$, requires, however, extension of the standard models to incorporate surface loss processes, especially surface plasmon and positronium creation. Accurate evaluation of the energy and θ dependence of these intensities for E<30eV probably requires incorporating the energy dependence of bulk inelastic processes into a bulk attenuation length, accounting for the removal of positrons from elastic channels by excitation of surface plasmons and by positronium formation, and possibly accounting for anisotropies in the atom scattering potentials or other effects in the diffraction process itself.

REFERENCES

a) Operated by Battelle Memorial Institute for the Department of Energy under Contract No. DE-AC06-76RLO 1830.

b) Present address: University of Texas at Arlington, Arlington, TX 76019.

c) Present address: AT&T Bell Laboratories, Murray Hill, NJ 07974.

d) Present address: Optron Systems, Bedford, MA 01730.

e) Work at Brandeis University supported by the National Science Foundation (Grant No. DMR-8820345).

[1] F. Jona, D.W. Jepsen, P.M. Marcus, I.J. Rosenberg, A.H. Weiss, and K.F. Canter, Solid State Commun. 36, 957 (1980).

[2] M.N. Read and D.N. Lowy, Surf. Sci. 107, L313(1981).

[3] A.H. Weiss, I.J. Rosenberg, K.F. Canter, C.B. Duke, and A. Paton, Phys. Rev. B 27, 867(1983).

[4] R. Mayer, C-S Zhang, K.G. Lynn, W.E. Frieze, F. Jona, and P. M. Marcus, Phys. Rev. B 35, 3102(1987).

[5] K.F. Canter, C.B. Duke, and A.P. Mills, Springer Series in Surf, Sci. 22(1990), in press.

[6] C.B. Duke, D.L. Lessor, T.N. Horsky, G. Brandes, K.F. Canter, P.H. Lippel, A.P. Mills, Jr., A. Paton, and Y. R. Wang, J. Vac. Sci. Technol. A7, 2030 (1989).

[7]T.N. Horsky, G.R. Brandes, K.F. Canter, C.B. Duke, S.F. Horng, A. Kahn, D.L. Lessor, A.P. Mills, Jr., A. Paton, K. Stevens, and K. Stiles, Phys. Rev. Lett 62, 1876(1989).

[8]C.B. Duke and D.L. Lessor, Surf. Sci. 225, 81(1990).

[9]C.B. Duke and C.W. Tucker, Jr., Surf. Sci. 15, 231 (1969).

[10]J. Oliva, Phys. Rev. B 21, 4909 (1980).

[11]G.C. Aers and J.B. Pendry, J. Phys. C: Solid State Phys. 15, 3725 (1982).

[12]J.B. Pendry, In Positron Solid State Physics, W. Brandt and A. Dupasquier, eds. (Soc. Italiana di Fiscia, Bologna, 1983), pp. 408-431.

[13]C.B. Duke, J.R. Anderson, and C.W. Tucker, Jr., Surf. Sci. 19, 117 (1970).

[14]K. Kambe, Surf. Sci 20, 213, (1970).

[15]M.N. Read, Solid State Commun. 47, 1 (1984).

[16]P.J. Jennings, Surf. Sci. 198, 180 (1988).

[17]K.F. Canter, G.R. Brandes, T.N. Horsky, P.H. Lippel, and A.P. Mills, Jr., in Atomic Physics with Positrons, edited by J.W. Humberston and E.A.G. Armour (Plenum, New York, 1987) pp. 153-160.

[18]T.N. Horsky, G.R. Brandes, K.F. Canter, P.H. Lippel, and A.P. Mills, Jr., Phys. Rev. B 40, 7898 (1989).

[19]D.A. Lieberman, J.T. Waber, and D.T. Cromer, Phys Rev. 137, A27 (1965).

[20]D.A. Lieberman, D.T. Cromer, and J.T. Waber, Comput. Phys. Commun. 2, 107 (1971).

[21]S.A. Lindgren, L. Wallden, J. Rundgren, and P. Westrin, Phys. Rev. B 29, 576 (1984).

[22]C.B. Duke and G.E. Laramore, Phys. Rev. B 2, 4765 (1970).

[23]C.B. Duke, N.O. Lipari, and V. Landman, Phys. Rev. B 8, 2454 (1973).

[24]I.J. Rosenberg, A.H. Weiss, and K.F. Canter, Phys. Rev. Lett. 44, 1139 (1980).

[25]E. Zanazzi and F. Jona, Surf. Sci. 62, 61 (1977).

[26]P.J. Feibelman, C.B. Duke, and A. Bagchi, Phys. Rev. B 5,2436(1972).

[27]K.F. Canter, A.P. Mills, Jr., and S. Berko, Phys. Rev. Lett. 33, 7 (1974).

[28]A.P. Mills, Jr. Phys. Rev. Lett. 41, 1828 (1978).

[29]D.W. Gidley, R. Mayer, W.E. Frieze, and K.G. Lynn, Phys. Rev. Lett. 8, 595 (1987).

[30]G.E. Laramore, C.B. Duke, and N.O. Lipari, Phys. Rev. B10, 2246 (1974).

TABLE 1. Multipliers f to scale calculated to experimental beam intensity curves, and single beam R-factors for the specular beam from the Cu(111) surface

Polar Angle j (deg)	Visually Determined Multiplier	Multiplier to Minimize Square Error	Single Beam R-factor
30	1.0	0.99	0.068
40	0.5	0.43	0.096
50	0.18	0.20	0.053
57	0.13	0.11	0.051

Figure Captions

Figure 1 Schematic diagram of the atomic geometry of Cu(111) [Panel (a)], the surface cell and its reciprocal lattice vectors $\underline{b}_1$, and $\underline{b}_2$, and the associated diffraction pattern [Panel(b)]. The length of the primitive surface unit cell vectors is taken to be $|a_x|=a_y| = 2.556$A. The beam positions are shown as if intersecting a hemispherical detector symmetrically positioned about the incident beam for 200 eV positrons at $\theta=25°$, $\phi=24°$.

Figure 2 Comparison of the measured (squares) and calculated specular beam intensities for positrons from Cu(111) at $\theta=30°$, $\phi=60°$. The solid curve is obtained using V_i=4eV. The cross-dashed curve is obtained using V_i from reference 10. Both curves are evaluated using a real (repulsive) inner potential of V_o=-2eV and are multiplied by a visually determined scaling factor for compatibility with the experimental measurements.

Figure 3 Comparison of measured (squares) and calculated specular beam intensities for positrons from Cu(111) at an azimuthal angle of $\phi=24°$. The cross-dashed curve is calculated using V_i=4eV and the solid curve using V_i from reference 10. Panel (a): $\theta=30°$ scaling factor = 1.0. Panel (b): $\theta=40°$, scaling factor = 0.5. Panel (c): $\theta=50°$, scaling factor = 0.18. Panel (d): $\theta=57°$, scaling factor = 0.13.

Figure 4 Same as Figure 3 but for a lower range of energies. Panel (a): $\theta=30°$ scaling factor = 0.78, V_o=-1eV. Panel (b): $\theta=40°$, scaling factor = 0.50. Panel (c): $\theta=50°$, scaling factor = 0.18. Panel (d): $\theta=57°$, scaling factor = 0.1, V_o=-1eV.

Figure 5 Calculated specular reflection intensities of positrons incident on a single Cu(111) monolayer. Solid curves are calculated for V_i=0.4eV and the dashed curves using inelastic mean free path λ=12.5A in Equation (1) or wave function attenuation length 25A. Panel (a): $\theta=30°$. Panel (b): $\theta=40°$. Panel (c): $\theta=50°$.

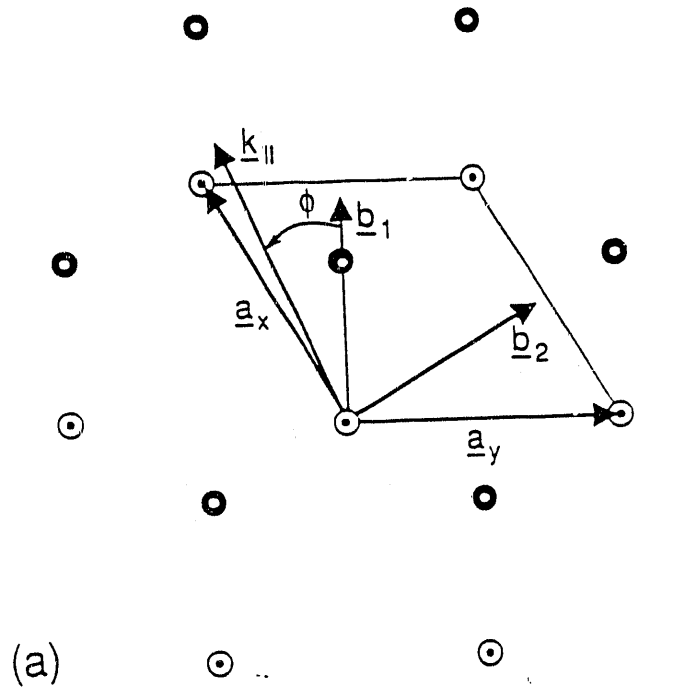

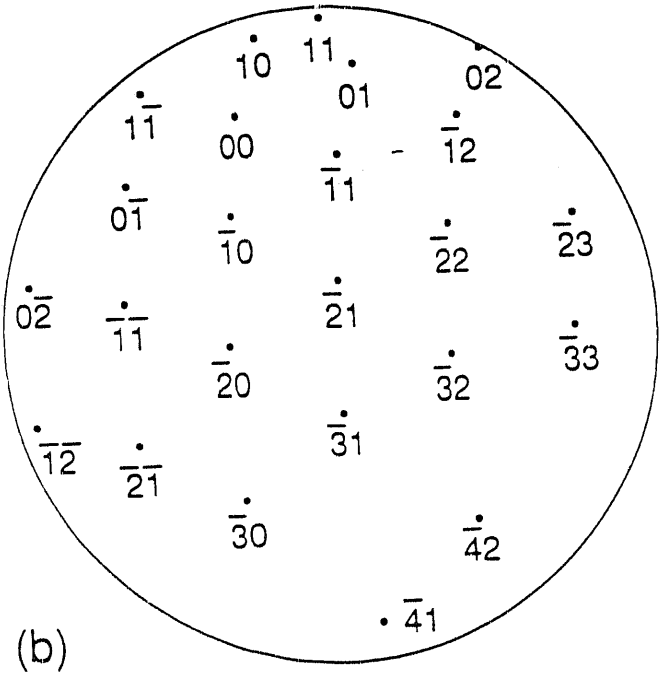

Fig. 1. Lessor, et al

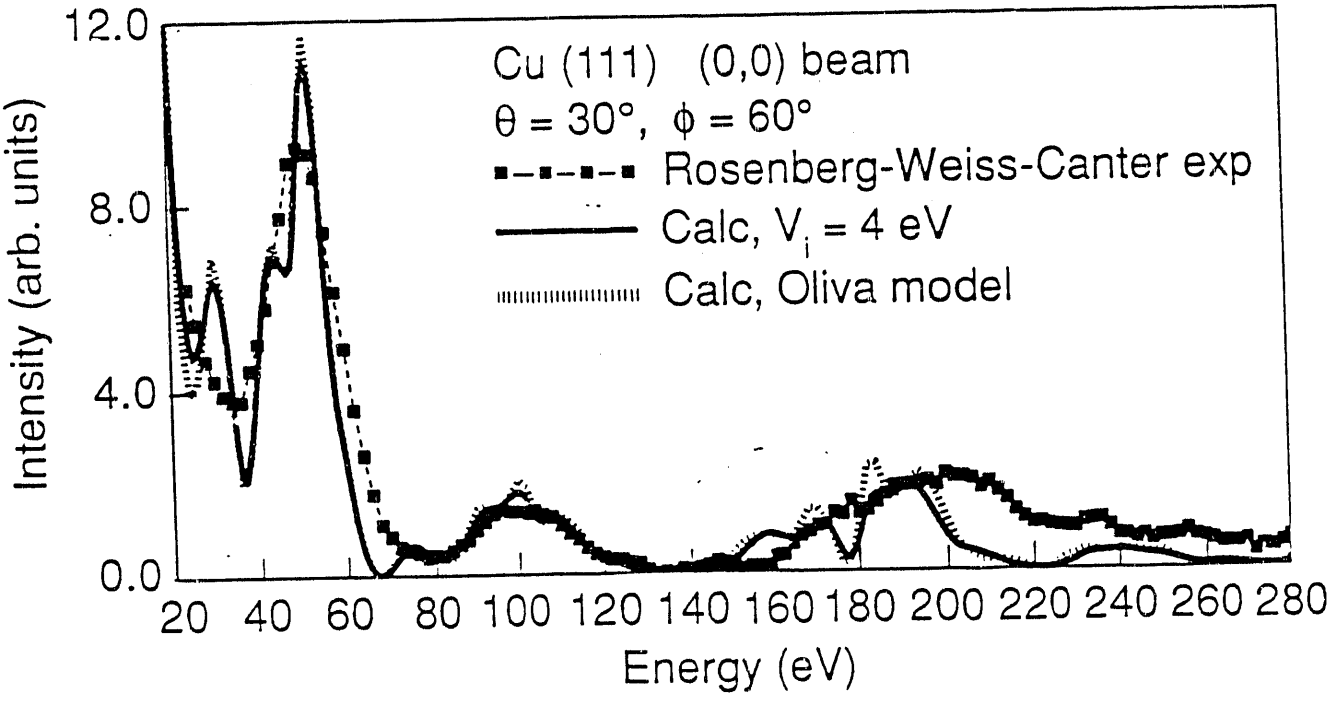

Fig. 2. Lessor, et al.

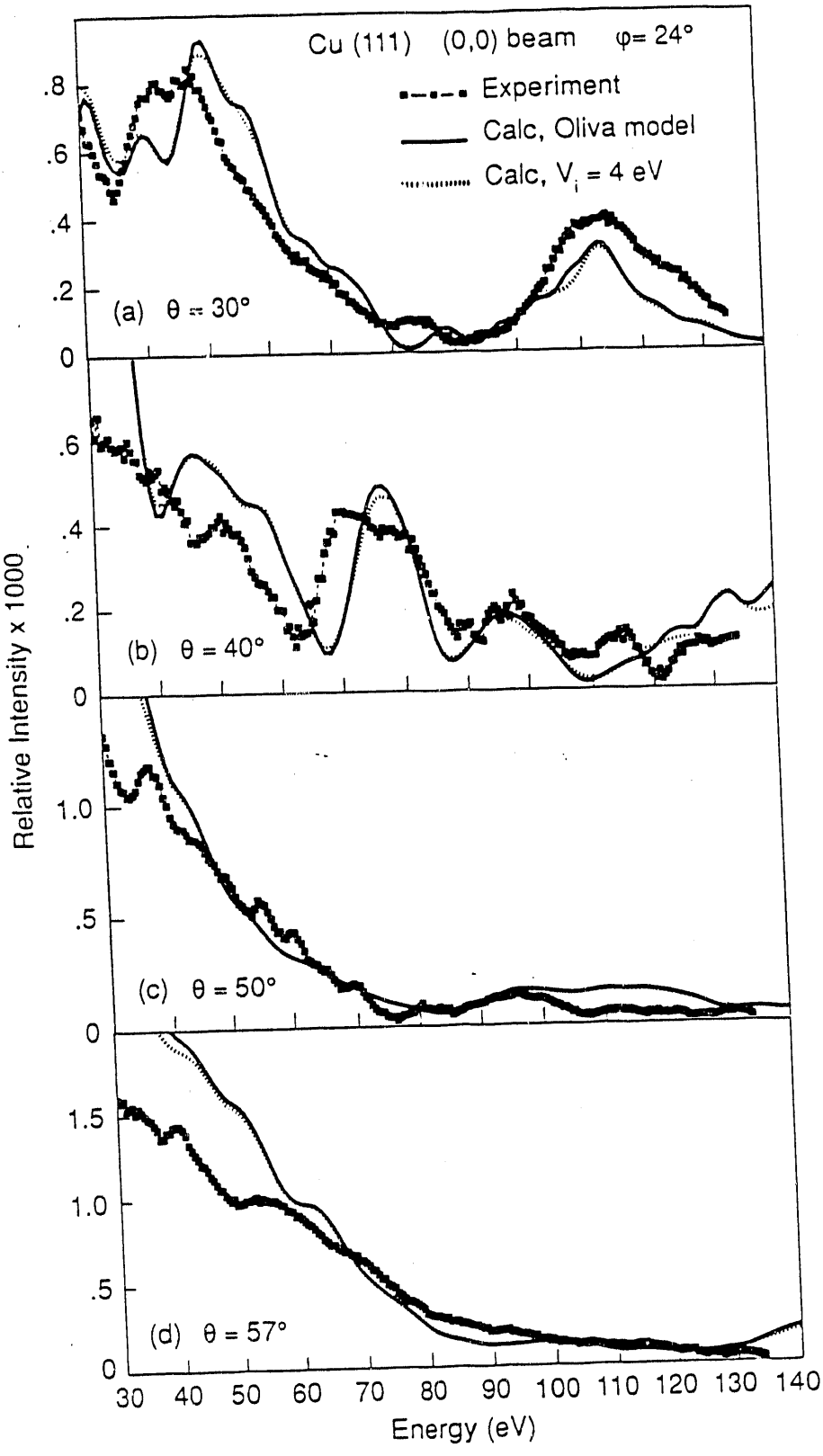

Fig. 3. Lessor, et al

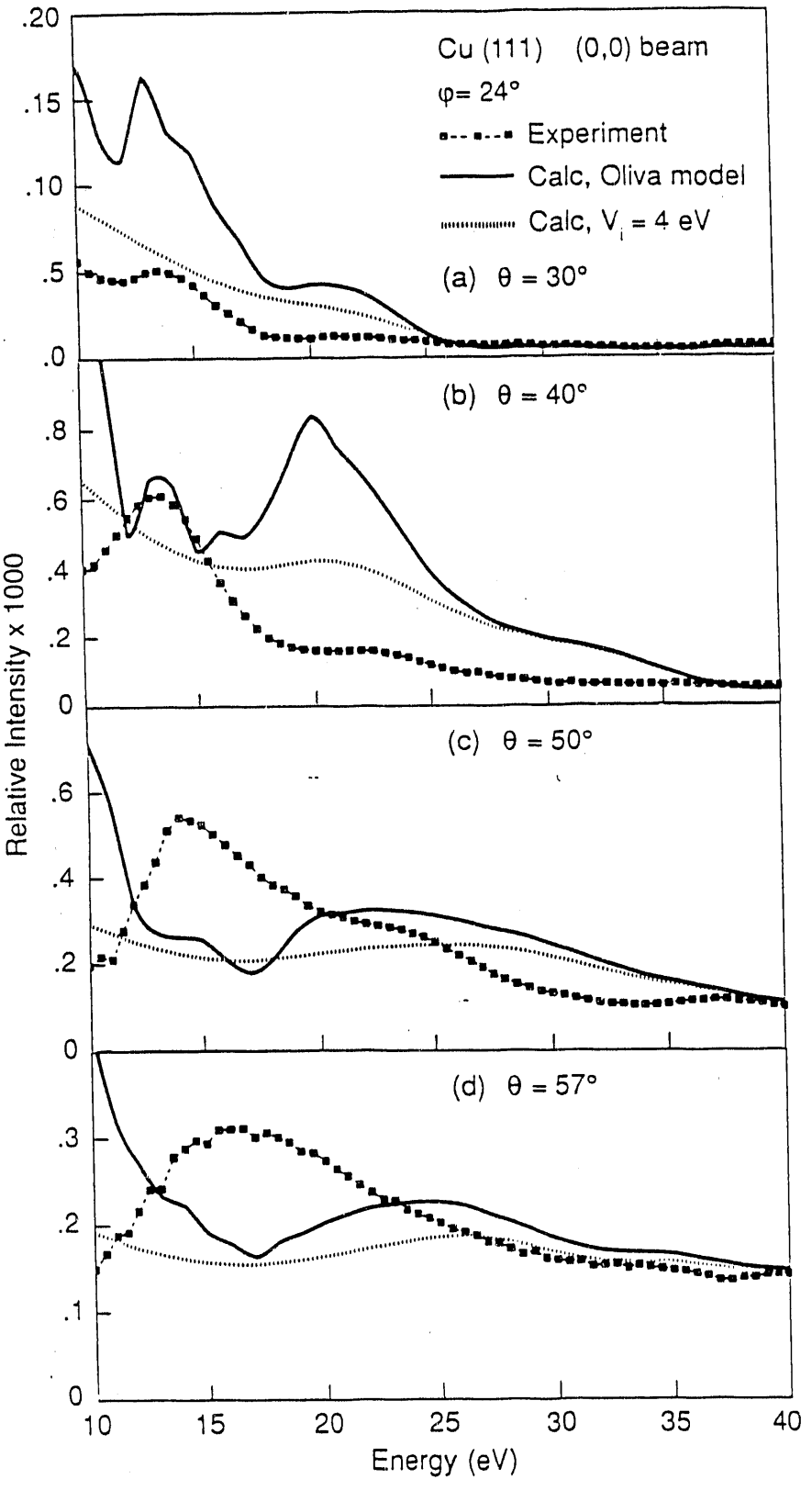

Fig. 4. Lessor, et al

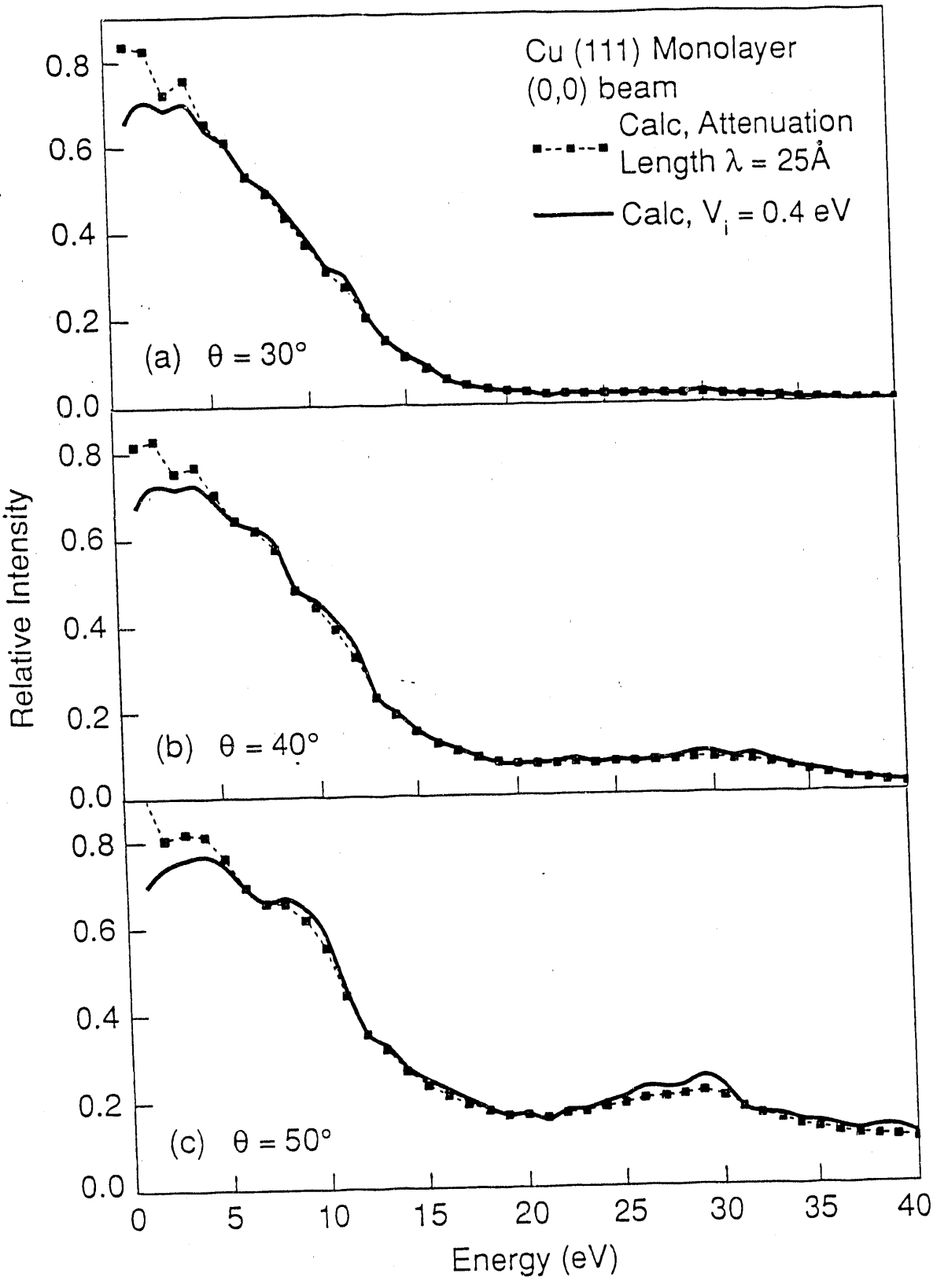

Fig. 5 Lessor, et al

END

DATE FILMED

02 / 28 / 91